Beverage Plant Research

ARTICLE

Open Access

https://doi.org/10.48130/bpr-0025-0041

Beverage Plant Research **2026**, 6: e011

Metabolic and transcriptome analysis reveals metabolite variation in fresh shoots of tea (*Camellia sinensis* 'Lingtou Dancong') under nitrogen-deficient conditions

Zihao Qiu[1], Ansheng Li[1], Xinyuan Lin[1], Jiyuan Yao[1], Yimeng Yang[1], Renjian Liu[1], Binmei Sun[1,2], Shaoqun Liu[1,2*] and Peng Zheng[1,2*]

[1] *College of Horticulture, South China Agricultural University, Guangzhou 510642, China*
[2] *Guangdong Provincial Engineering Technology Research Center for Southern Specialty Tea, Guangzhou 510642, China*
* Correspondence: scauok@scau.edu.cn (Liu S); zhengp@scau.edu.cn (Zheng P)

Abstract

Although nitrogen deficiency severely constrains tea's quality, the systemic adaptation mechanisms of new shoots to N deficiency remain poorly understood. Using integrated physiology, metabolomics, and transcriptomics, we discovered that nitrogen-stressed tea shoots (*Camellia sinensis* 'Lingtou Dancong') deploy a phased acclimation strategy. This strategy precipitated a quality trade-off, marked by a very hihg phenol-to-amino acid ratio and a dramatic 66.67% decline in theanine. This metabolic shift was driven by the accumulation of key stress metabolites, namely jasmonoyl-L-isoleucine (JA-Ile) (20.19-fold), luteolin (~8-fold), and γ-aminobutyric acid (GABA) (3.63-fold, which were further regulated by three core transcriptional modules: bZIP11/23/bHLH149-HCT (luteolin synthesis), bZIP11/23/bHLH149-MYC2-JAZ (JA-Ile accumulation), and RAV2/bZIP53/ATH7-ASNS (GABA production). Our study thus reveals a coordinated gene–metabolite network that orchestrates adaptation to nitrogen deficiency in tea shoots, providing mechanistic insights and practical targets for improving nitrogen use efficiency.

Citation: Qiu Z, Li A, Lin X, Yao J, Yang Y, et al. 2026. Metabolic and transcriptome analysis reveals metabolite variation in fresh shoots of tea (*Camellia sinensis* 'Lingtou Dancong') under nitrogen-deficient conditions. *Beverage Plant Research* 6: e011 https://doi.org/10.48130/bpr-0025-0041

Introduction

The synthesis of metabolites is a crucial aspect of nitrogen utilization in tea plants. These metabolites play a key role in the growth and development, stress tolerance, and quality of tea leaves[1]. The chlorophyll in tea leaves plays a key role in photosynthesis, improving the plant's photosynthetic efficiency, and nitrogen is essential for the synthesis of chlorophyll[2]. In terms of stress resistance, nitrogen boosts flavonoid synthesis and regulates plant hormones, thereby improving tolerance to environmental stresses[3]. The nitrogen supply also significantly impacts the synthesis of key compounds in tea leaves, such as amino acids, tea polyphenols, and caffeine[4]. Proper nitrogen fertilization supports amino acid accumulation, which enhances the taste quality of tea. However, excessive or poorly timed nitrogen application can disrupt the balance between amino acids and tea polyphenols, negatively affecting the aroma and flavor of the tea[5].

Tea plants respond to nitrogen-deficient conditions through various mechanisms, including the regulation of auxin synthesis to promote lateral root formation and the control of secondary metabolite synthesis and transport. These adaptive responses help tea plants maintain growth under low nitrogen conditions and quickly restore normal metabolic activities once nitrogen is available again. Current research shows that under nitrogen-deficient conditions, tea plants regulate the synthesis and transport of auxin to control root growth[6]. In addition, under nitrogen-deficient conditions, tea plants also regulate the synthesis of secondary metabolites, especially those promoting the accumulation of phenylpropanoids and organic acids in the leaves[7]. Research suggests that under long-term nitrogen-deficient conditions, the cell wall metabolism and secondary metabolism of nitrogen-tolerant tea genotypes remain stable, and lignin synthesis genes may serve as candidate genes for breeding nitrogen-tolerant tea varieties[8]. Moreover, under nitrogen-deficient conditions, various flavonoids accumulate in the new shoots, which is associated with the high expression of core genes such as *flavanone 3-dioxygenase* (*F3H), flavone synthase (FNS), UDPG-flavonidsglucosyltransferase (UFGT), basic helix-loop-helix transcription factor 35/36 (bHLH35, and bHLH36)*[9]. In the roots, the accumulation of flavonoids and the suppression of amino acid synthesis are the main responses of tea plants to nitrogen-deficient conditions. Several enzyme-coding genes involved in the synthesis of theanine, such as theanine synthetase, glutamate dehydrogenase, and glutamine synthetase, are inhibited at the transcriptional or protein level under nitrogen-deficient conditions[10]. Tea's amino acid transport proteins *Cs*AAP1, *Cs*AAP2, and *Cs*AAP6 may participate in the response of tea plants to nitrogen-deficient conditions by regulating the transport of amino acids from the roots to new shoots and from source tissues to storage tissues[11]. The capacity for nitrogen absorption and transport, as well as the ability to convert key amino acids such as glutamate and γ-aminobutyric acid (GABA), may enhance the adaptability of tea plants during nitrogen recovery[12].

Currently, most studies focus on the response of tea plant roots to nitrogen-deficient conditions, whereas research on changes in the quality of new shoots under sustained nitrogen-deficient conditions and the core biomarkers related to their adaptive mechanisms is still lacking. Therefore, this study aimed to reveal the impact of nitrogen-deficient conditions on the quality of new shoots by setting different nitrogen-deficiency treatment time points (0, 7, 15, and 30 d) and to identify the transcription factor–gene–metabolite regulatory modules that are responsive to nitrogen-deficient conditions. Future research on the mechanisms by which these modules

affect metabolites will provide important references for screening and breeding tea varieties with high nitrogen use efficiency.

Materials and methods

Plant material and experimental design

Two-year-old clonal cuttings of *Camellia sinensis* 'Lingtou Dancong' were hydroponically cultivated following an initial 3-month acclimatization period in a complete nutrient solution. Plants were maintained in a controlled environment growth chamber under a 14/10 h light/dark photoperiod, with a light intensity of 270 μmol·m^{-2}·s^{-1}, a temperature of 24–26 °C, a relative humidity of 60%–70%, and continuous aeration. The nutrient solution, adapted from Liu et al.[13], was renewed every 7 d and its pH was adjusted to 5.0 ± 0.2. The full nutrient solution contained the macronutrients $(NH_4)_2SO_4$ (1.125 mM), $Ca(NO_3)_2$ (0.375 mM), KH_2PO_4 (0.1 mM), K_2SO_4 (0.5 mM), $MgSO_4$ (0.4 mM), and $CaCl_2$ (0.3 mM) and the micronutrients H_3BO_3 (10 μM), $MnSO_4$ (1.5 μM), $ZnSO_4$ (1.0 μM), $CuSO_4$ (0.2 μM), Na_2MoO_4 (0.07 μM), and Fe-EDTA (6.3 μM).

To initiate the nitrogen-deficient (ND) treatment, acclimated seedlings were transferred to a nutrient solution devoid of nitrogen sources (i.e., without $(NH_4)_2SO_4$ and $Ca(NO_3)_2$). New shoots (one bud with two leaves) were randomly sampled at 0 (CK, control), 7 (Nd1), 15 (Nd2), and 30 (Nd3) days after initiating the ND treatment for subsequent analysis (Supplementary Fig. S1).

Physiological and biochemical profiling

Chlorophyll and carotenoid contents were determined spectrophotometrically according to Lichtenthaler[14] and Wang et al.[15] (three biological replicates with three technical replicates). Elemental analysis was performed using an Elementar Rapid N Exceed analyzer[9] with 30-mg aliquots (protein conversion factor: 6.25[16]) and an Elementar Vario EL cube[17] with 5-mg aliquots (four biological replicates). Total tea polyphenols (GB/T 8313) and total free amino acids (GB/T 8314) were quantified with four biological replicates. Theanine, caffeine, and catechin monomers were analyzed by high-performance liquid chromatography (HPLC) in the ultraviolet–visible (UV/vis) range[18] with calibration curves (Supplementary Table S1; three biological replicates). Malondialdehyde (MDA) (Solarbio BC0020) and soluble sugar (Solarbio BC0030) contents were assessed with three biological replicates (Supplementary Table S1). Detailed experimental procedures are provided in Supplementary Method 1.

Analysis of volatile components and odor activity values

Volatile compounds were analyzed according to the method of Chen et al.[19] using headspace solid-phase microextraction coupled with gas chromatography–mass spectrometry (GC-MS). Compound identification was performed by comparing retention indices and mass spectra with the NIST database. Odor activity values (OAVs) were calculated as the ratio of a compound's concentration to its odor threshold according to the referenced methodology[20]. Detailed experimental procedures are provided in Supplementary Method 1.

Widely targeted metabolomics and differential analysis

Nonvolatile metabolites were profiled using a widely targeted metabolomics approach by ultrahigh-performance liquid chromatography–tandem mass spectroscopy (UPLC-MS/MS), following the methodology described by Wang et al.[21] with assistance from Wuhan MetWare Biotechnology Co., Ltd. Differential accumulated metabolites (DAMs) were screened using the MVDB database, with selection criteria of variable importance in projection (VIP) > 1 and $\log_2$ fold change FC ≥ 1.0 for pairwise comparisons, or VIP > 1 and $p < 0.05$ for multi-group comparisons. All orthogonal partial least squares discriminant analysis (OPLS-DA) models were validated with 200 permutation tests to prevent overfitting. Analyses were performed in three biological replicates (Supplementary Tables S2–S5). Detailed experimental procedures are provided in Supplementary Method 1.

Transcriptome sequencing and differential expression analysis

Transcriptome analysis was conducted following the methodology of Lin et al.[22]. Briefly, total RNA was extracted from new shoot samples, and sequencing libraries were prepared and sequenced on an Illumina HiSeq X Ten platform. Quality-controlled reads were aligned to the *Camellia sinensis* cv. Shuchazao reference genome using HISAT2. Gene expression levels were quantified as fragments per fragments per kilobase of feature per million mapped reads (FPKM), and differentially expressed genes (DEGs) were identified using the DESeq2 package with a threshold of $|\log_2(FC)| \geq 1$ and false discovery rate (FDR) < 0.05 (Supplementary Tables S6–S9). Functional enrichment of DEGs was analyzed on the basis of Kyoto Encyclopedia of Genes and Genomes (KEGG) (www.genome.jp/kegg) pathway annotations[23,24]. The analysis included three biological replicates per treatment group. Detailed experimental procedures are provided in Supplementary Method 1.

Co-expression network construction and quantitative real-time polymerase chain reaction validation

Gene co-expression networks were constructed using weighted gene co-expression network analysis (WGCNA) implemented on the Metwarecloud platform (https://cloud.metware.cn) with the WGCNA R package (v1.71), following established methodologies for identifying hub genes under nitrogen stress conditions. The network was built from 8,828 DEGs and 22 core metabolites using Pearson's correlation with the parameters of power = 18 and minimum module size = 850, and visualized in Cytoscape (v3.9.1). For experimental validation, quantitative real-time polymerase chain reaction (qRT-PCR) was performed according to established protocols[5] using RNA extracted with a Magen Plant Total RNA Extraction Kit. cDNA was synthesized with an EZBioscience reverse transcription kit, and amplification was conducted on a BIO-RAD CFX Opus 384 system using *CsActin (TEA019484)* as the reference gene. Gene expression was quantified via the $2^{-\Delta\Delta C_T}$ method with three biological replicates (Supplementary Tables S10 and S11).

Statistical analysis

Data are expressed as the mean ± standard deviation (SD). Normality and homogeneity of variances were verified using Shapiro–Wilk and Hartley's tests, respectively. Differences between groups were assessed by one-way analysis of variance (ANOVA) followed by Duncan's test ($p < 0.05$) in SPSS 27. Multivariate analyses included principal coordinate analysis (PCA) (R prcomp function) and OPLS-DA (SIMCA 14.1). Heatmaps were generated using TBtools, and general graphing was performed with GraphPad Prism 9.5.

Results

Physiological and biochemical responses to nitrogen deficiency

Nitrogen deficiency induced a systematic physiological and metabolic reprogramming in new shoots of tea plants. This adaptive response was initiated by alterations in the elemental stoichiometry (Fig. 1a, Supplementary Table S12): Nitrogen content decreased significantly (15.96%–21.22%) at the early deficiency stage (Nd1), accompanied by an increase in the carbon–nitrogen ratio (28.15%) and a substantial reduction in sulfur content. These shifts collectively reflect a strategic reallocation of resources under nitrogen limitation, moving the metabolic emphasis away from nitrogen-dependent growth toward carbon-based stress responses. At the physiological level (Fig. 1b, Supplementary Table S13), this reprogramming was manifested as photosynthetic adjustment and maintained oxidative homeostasis. A sustained decline in chlorophyll indicated reduced photosynthetic capacity, whereas the compensatory accumulation of carotenoids in the later stages,

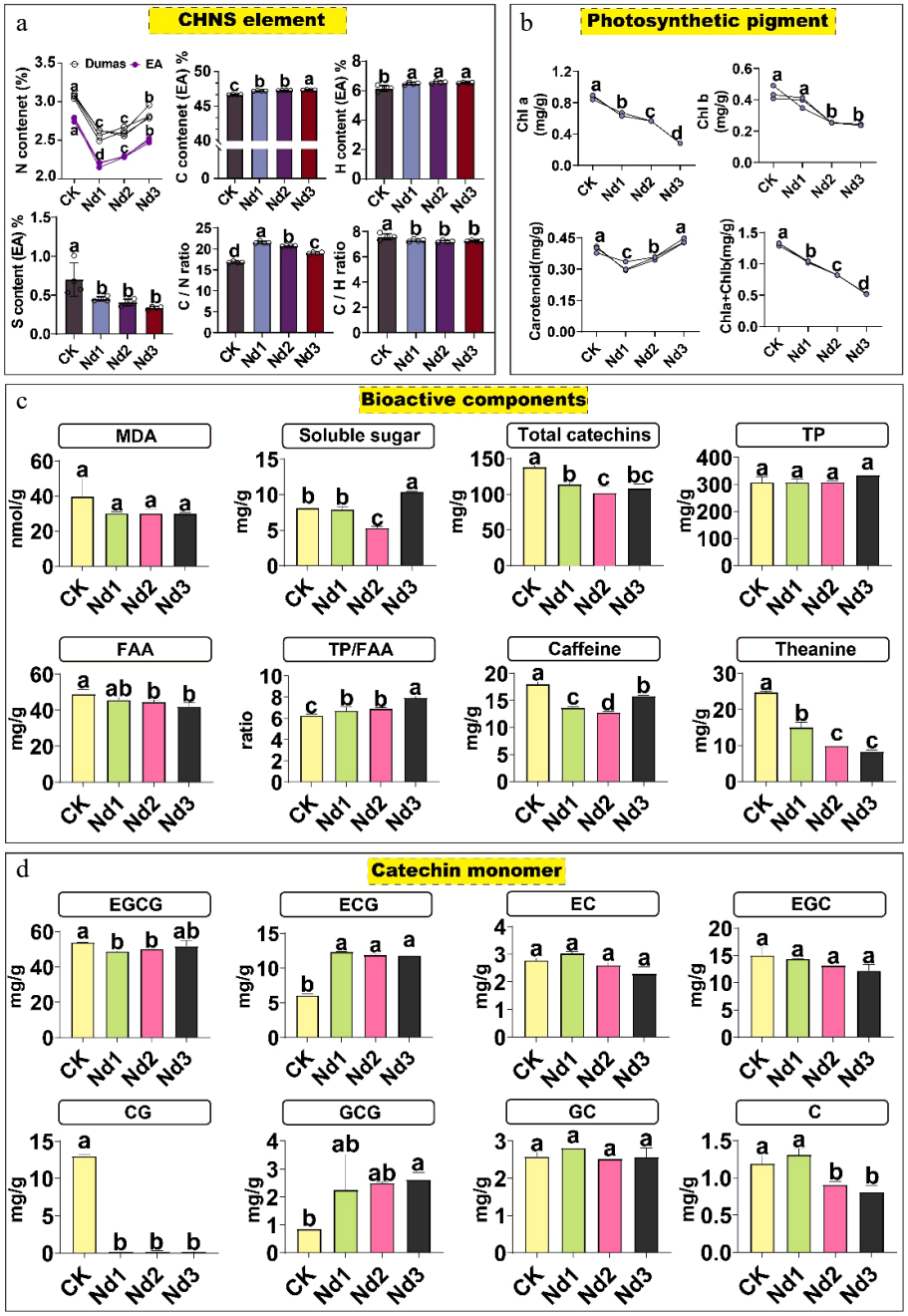

Fig. 1 Physiological and biochemical changes in tea new shoots during nitrogen deficiency. Plants were subjected to deficiency treatments for 0 (CK, control), 7 (Nd1), 15 (Nd2), and 30 (Nd3) days. (a) Analysis of carbon, hydrogen, nitrogen, and sulfur elements. (b) Analysis of photosynthetic pigments. (c) Analysis of bioactive components. (d) Analysis of catechin monomers. The data represent the mean ± SD (n = 4) for soluble sugar content (n = 3). Different letters indicate significant differences at $p < 0.05$ determined by Duncan's multiple range test. Malondialdehyde, MDA; total free amino ccid content, FAA; total polyphenol content, TP; catechin, C; epicatechin, EC; gallocatechin, GC; epigallocatechin, EGC; epicatechin gallate, ECG; gallocatechin gallate, GCG; catechin gallate, CG; epigallocatechin gallate, EGCG.

together with stable MDA levels, demonstrated the activation of photoprotective and antioxidant mechanisms that preserved membrane integrity, prioritizing survival under stress conditions (Fig. 1c, Supplementary Table S13).

This physiological and elemental reconfiguration further led to a marked remodeling of quality-related components. Key nitrogen-containing compounds, including theanine, caffeine, and total catechins, decreased significantly (theanine content fell by 66.67% at the Nd3 stage), whereas the phenol–amino acid ratio (TP/AA) consistently increased (Fig. 1c, Supplementary Table S13). This carbon for nitrogen trade-off illustrates a metabolic shift that diverts resources from quality-related biosynthesis toward stress adaptation. Notably, gallated catechins (gallocatechin gallate [GCG] epigallocatechin gallate [ECG]) accumulated markedly under nitrogen deficiency, contrasting with the general decline in other catechin monomers, suggesting a potential specialized role in antioxidant defense or stress mitigation (Fig. 1d, Supplementary Table S13).

In summary, new shoots of tea plants deploy a hierarchical adaptive strategy—progressing from elemental rebalancing to photosynthetic adjustment and finally quality component remodeling—centered on a carbon compensation mechanism, thereby achieving metabolic equilibrium and sustained viability under nitrogen-deficient conditions.

Effects of nitrogen-deficient conditions on volatile components and their dynamic changes

Nitrogen deficiency induced systematic and dynamic restructuring of volatile organic compounds (VOCs) in new shoots of tea. A total of 37 VOCs were identified, with aldehydes, alcohols, and esters constituting the predominant chemical classes (Fig. 2a, c, Supplementary Table S14). Under nitrogen stress, their combined abundance increased from 78.0% in CK to 84.6% in Nd1, indicating intensified synthesis of these aroma-related metabolites (Fig. 2a). Notably, aldehydes exhibited the most significant accumulation, rising from 39.2% in CK to 54.7% in Nd1, accompanied by a 79.3% increase in total aldehyde content, suggesting a shift toward aldehyde-dominated volatile profiles (Fig. 2a). This metabolic reprogramming featured distinct compositional and temporal dynamics. Key aldehydes, including (E)-2-hexenal (grassy notes) and decanal (fruity notes), increased markedly by 42.88% and 138.11%, respectively, peaking at the Nd1 stage. Conversely, several alcohols and esters declined, such as linalool (floral) and geraniol (floral-fruity), which decreased by 11.42% and 13.25%, respectively, implying a reduction in floral aroma characteristics. Ketones showed compound-specific responses, with geranylacetone increasing by 111.88%, whereas esters fluctuated dynamically (Fig. 2b).

Multivariate statistical analyses substantiated the significant alteration in the composition of VOCs under nitrogen deficiency. Teh PCA and OPLS-DA models confirmed a clear separation between nitrogen-deficient treatments and CK, with the most pronounced difference observed at the Nd1 stage (Fig. 2d–f). VIP analysis identified 11 discriminative aroma compounds, and integration with OAVs (OAV ≥ 1) further pinpointed seven characteristic volatiles that define the nitrogen-deficient aroma signature. (E)-2-Hexenal emerged as the most influential marker (VIP = 2.89; OAV = 10.3–17.7), followed by decanal, geranylacetone, and linalool, which also exhibited high OAVs (Fig. 2g, Table 1).

To sum up, the transition in VOC profiles reflects a strategic reallocation of metabolic resources under nitrogen limitation. The conspicuous accumulation of aldehydes, particularly (E)-2-hexenal, coupled with the decline in key floral alcohols, indicates a shift from floral-fruity notes toward green, fatty, and fruity aroma characteristics. This 'green shift' is consistent with an adaptive response, wherein carbon flux is redirected toward defense-related volatiles at the expense of quality-associated aromas. The seven identified characteristic volatiles, including grassy (E)-2-hexenal, floral-fruity geraniol and geranylacetone, and fruity decanal, serve as functional markers for aroma remodeling under nitrogen stress. Their dynamic changes not only signify a biochemical response but also sensorially define the aroma identity of nitrogen-deficient tea shoots, offering measurable targets for quality assessment and metabolic regulation.

Integrated analysis of metabolic reprogramming under nitrogen deficiency

Nitrogen deficiency induced a comprehensive metabolic reorganization in tea shoots, characterized by dynamic changes in both primary and secondary metabolism. Multivariate analysis revealed that the number of differentially accumulated metabolites (DAMs) increased with prolonged nitrogen stress, with the CK vs. Nd3 comparison showing the most significant changes (Fig. 3a–c). Flavonoids, phenolic acids, amino acids, and their derivatives constituted the majority of DAMs across all comparison groups, accounting for 40.11%–44.63% of all metabolites (Fig. 3d–e). K-means clustering of 711 DAMs identified nine distinct response patterns, with Cluster 5 (50 metabolites) showing significant accumulation under stress, primarily flavonoids (10/50), lipids (9/50), and phenolic acids (9/50), whereas Cluster 8 (74 metabolites) exhibited marked decreases, including flavonoids (32/74), amino acids (7/74), and saccharides (6/74) (Supplementary Fig. S2).

KEGG enrichment analysis revealed these metabolites were predominantly associated with six major metabolic categories: Plant hormone metabolism, lipid metabolism, amino acid metabolism, carbohydrate metabolism, flavonoid metabolism, and chlorophyll metabolism (Fig. 3f). Notably, the flavonoid biosynthesis pathways were significantly enriched but showed negative differential abundance scores, indicating general suppression under nitrogen deficiency. Conversely, the plant hormone signal transduction and α-linolenic acid metabolism pathways exhibited positive scores, suggesting their activation under stress conditions. The sulfur relay system related to chlorophyll metabolism was significantly suppressed, consistent with the observed photosynthetic alterations.

Analysis of DEGs in nitrogen-deficient new shoots

Nitrogen deficiency triggered an extensive transcriptional reprogramming in new shoots of tea, showing strong temporal dynamics and close coordination with metabolomic changes. As shown in Supplementary Tables S15 and S16, all RNA samples used for transcriptome sequencing demonstrated high integrity. The raw sequencing data thus generated were of high quality. In total, 669 DEGs were consistently differentially expressed across all treatment stages, representing a core set of nitrogen stress-responsive transcripts (Supplementary Fig. S4). Among the 561 differentially regulated transcription factors (TFs), members of the bHLH (51), MYB (50), and AP2/ERF (43) families were most abundant, suggesting their potential roles in regulating the secondary metabolite pathways observed in the metabolic profiles (Supplementary Fig. S5).

Functional annotation revealed that nitrogen deprivation primarily affected chromatin organization, cell wall biosynthesis, and carbohydrate metabolism (Supplementary Fig. S6). The enrichment

of cell wall-related pathways supports the metabolic observations of structural reinforcement under stress. KEGG analysis demonstrated time-dependent pathway activation (Supplementary Fig. S7): Flavonoid/flavonol biosynthesis was induced at the Nd1 stage, corresponding to the early accumulation of luteolin and other flavonoids detected metabolically. By the Nd2 stage, terpenoid biosynthesis pathways were upregulated, consistent with the observed changes in volatile terpenes. Crucially, the persistent activation of plant hormone signaling pathways throughout the treatment period indicates the transcriptional basis for the massive

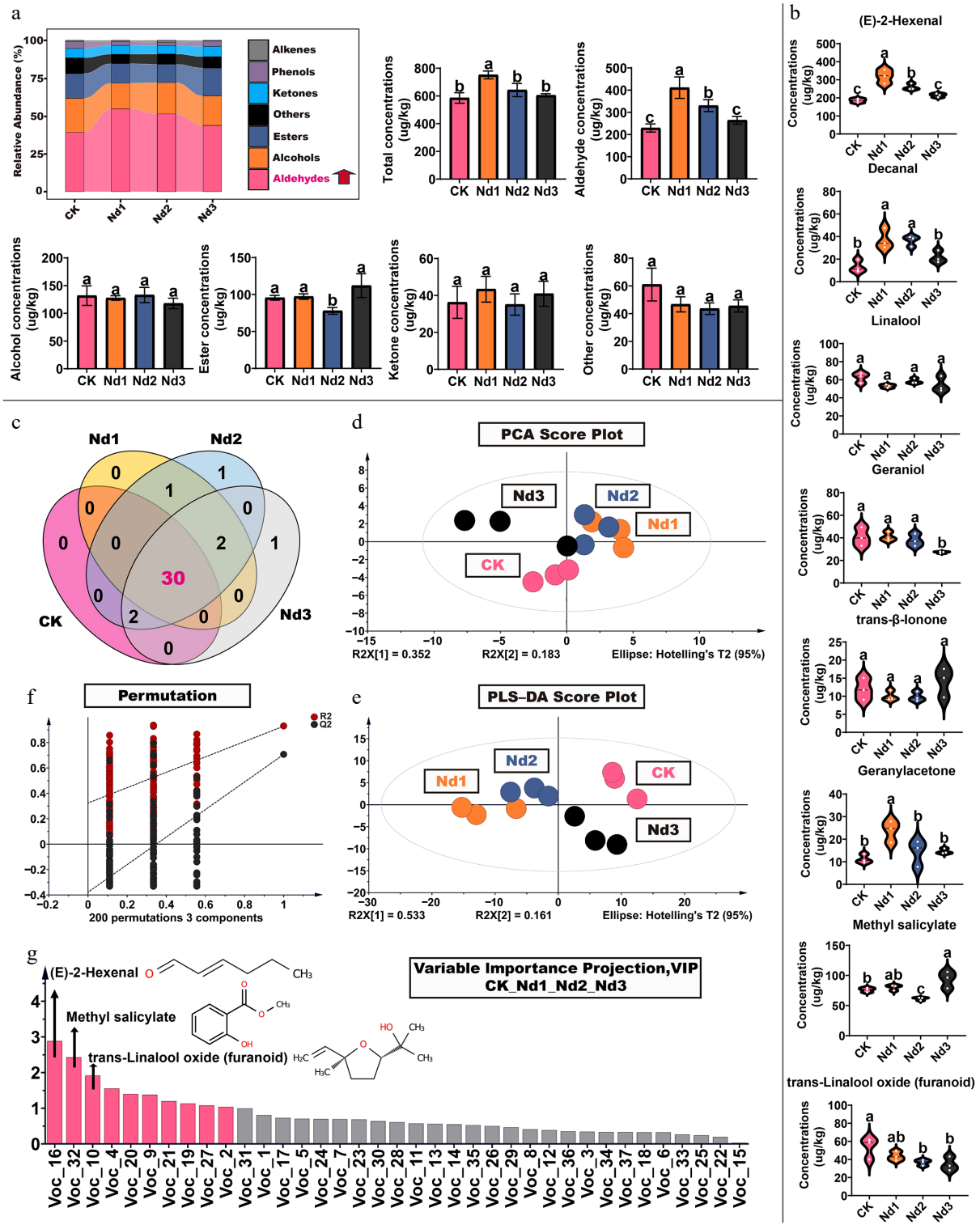

Fig. 2 Changes in volatile component levels in new shoots of tea under nitrogen deficiency treatment. (a) Proportion of volatile components: total concentration, aldehydes, alcohols, esters, ketones, and other volatile compounds concentrations. (b) High concentration volatiles. (c) Venn diagram of volatile component counts. (d) Principal component analysis; (e) 200 permutation tests. (f) Partial least squares analysis. (g) Projection of important variables. The data represent the mean ± SD (n = 3). Different letters indicate significant differences at $p < 0.05$ determined by Duncan's multiple range test.

Table 1. Seven key aroma compounds (OAV ≥ 1, VIP ≥ 1) under the nitrogen deficiency treatment.

No.	Volatile compounds	OT (μg/L)	OAV				VIP	Odor description
			CK	Nd1	Nd2	Nd3		
Voc_2	Linalool	0.6	104.3	88.1	98.4	90.5	1.04	Floral
Voc_4	Geraniol	3.2	12.7	12.8	11.8	8.5	1.56	Floral, fruity
Voc_16	(E)-2-hexenal	18	10.3	17.7	14.4	11.9	2.89	Green
Voc_19	(E,E)-2,4-heptadienal	0.032	308.1	597.1	314.8	194.2	1.14	Fatty, floral
Voc_20	Decanal	0.1	133.3	372.7	362.5	216.7	1.41	Fruity
Voc_27	Geranylacetone	0.06	186.6	395.4	237.4	243.1	1.08	Floral, fruity
Voc_32	Methyl salicylate	40	1.9	2.0	1.5	2.3	2.43	Minty

VOC, volatile organic compound; OT, odor threshold in water (see the references in Supplementary Table S14); OAV, odor activity value.

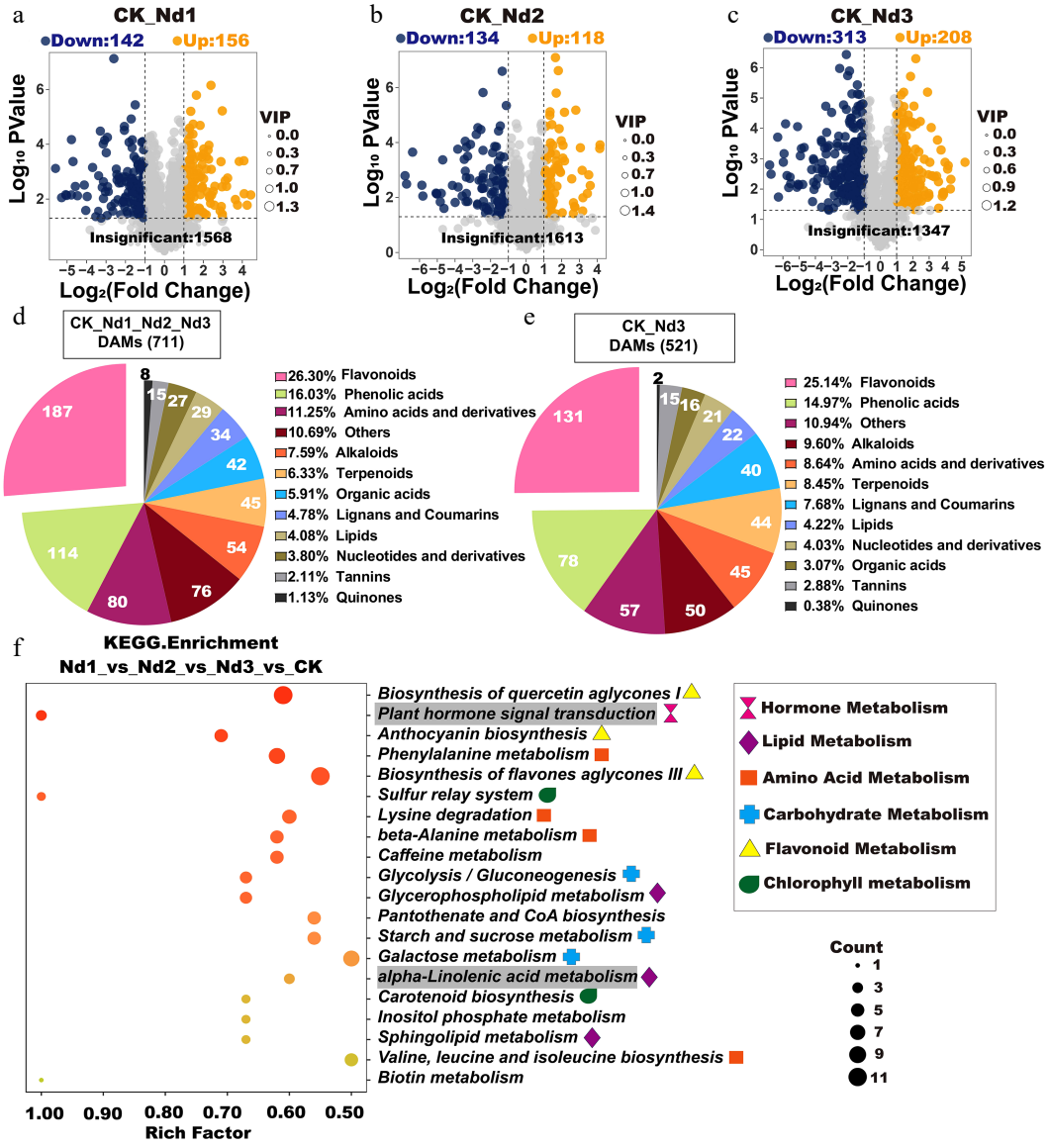

Fig. 3 Analysis of differential accumulation metabolites (DAMs) in new shoots under the nitrogen deficiency treatment. (a–c) Volcano plots of DAMs. Each point represents a metabolite: Blue = downregulated), orange = upregulated, and gray = nonsignificant. The *x*-axis indicates the $\log_2$FC in relative abundance, the *y*-axis shows $\log_{10}$ *p*-values, and the point size corresponds to VIP values. Higher *y*-axis values denote stronger statistical confidence. (d) The categorical distribution of shared DAMs across four treatment groups. Pie chart sectors represent distinct metabolite classes, with numeric labels indicating the absolute counts per category and percentages, reflecting their proportion relative to total DAMs. (e) Types, quantities, and proportions of DAMs shared between the CK and Nd3 groups. (f) KEGG enrichment analysis of the CK, Nd1, Nd2, and Nd3 comparison groups. Gray-shaded pathways indicate significant enrichment in all pairwise comparisons (validated in Supplementary Fig. S3).

accumulation of jasmonoyl-L-isoleucine (JA-Ile) and other hormone-related metabolites (Supplementary Fig. S8). This integrated analysis reveals that tea shoots orchestrate transcriptional reprogramming to prioritize defense-oriented metabolism under nitrogen limitation, with specific TF families and metabolic pathways working in coordination to reconfigure the metabolic landscape.

Metabolic reprogramming of flavonoid biosynthesis under nitrogen deficiency

Integrated transcriptomic and metabolomic analyses revealed extensive reprogramming of the flavonoid biosynthesis pathway in tea shoots under nitrogen deficiency, with numerous DAMs and DEGs identified (Fig. 4). To elucidate the regulatory mechanisms, we focused on 11 key DAMs and 52 DEGs (FPKM > 10) involved in flavonoid and phenylpropanoid metabolism. Our analysis identified luteolin as a key responsive metabolite, showing the most pronounced accumulation, reaching 8.16-, 8.36-, and 7.47-fold of the control levels at the Nd1, Nd2, and Nd3 stages, respectively (Supplementary Fig. S9). This marked increase, along with the moderate accumulation of dihydromyricetin and ± gallocatechin, suggests that tea plants enhance the synthesis of these antioxidant flavones to mitigate nitrogen limitation-induced oxidative stress. The process is driven by the upregulation of *CYP75B1* and *HCT*: The expression of *CYP75B1_CSS0035984* increased from 11.65 to 41.25 at the Nd1 stage, whereas the expression of *HCT_CSS0047836* and *HCT_CSS0009318* rose substantially by the Nd3 stage. Functionally, CYP75B1 catalyzes the 3'-hydroxylation of flavones, a critical step converting naringenin to luteolin, whereas HCT supports metabolic flux by regulating phenylpropanoid precursor availability. Overall, flavonoid metabolism underwent targeted rather than global reprogramming, with carbon flux redirected toward aglycone flavonoids (e.g., luteolin) potentially at the expense of branches such as acylated glycosides. The coordinated upregulation of core structural genes (*PAL, CHS, CHI, DFR*) and specific induction of CYP75B1 collectively promoted the synthesis of defense-effective flavones, reflecting an adaptive strategy of metabolic restructuring to optimize resource allocation under nitrogen stress.

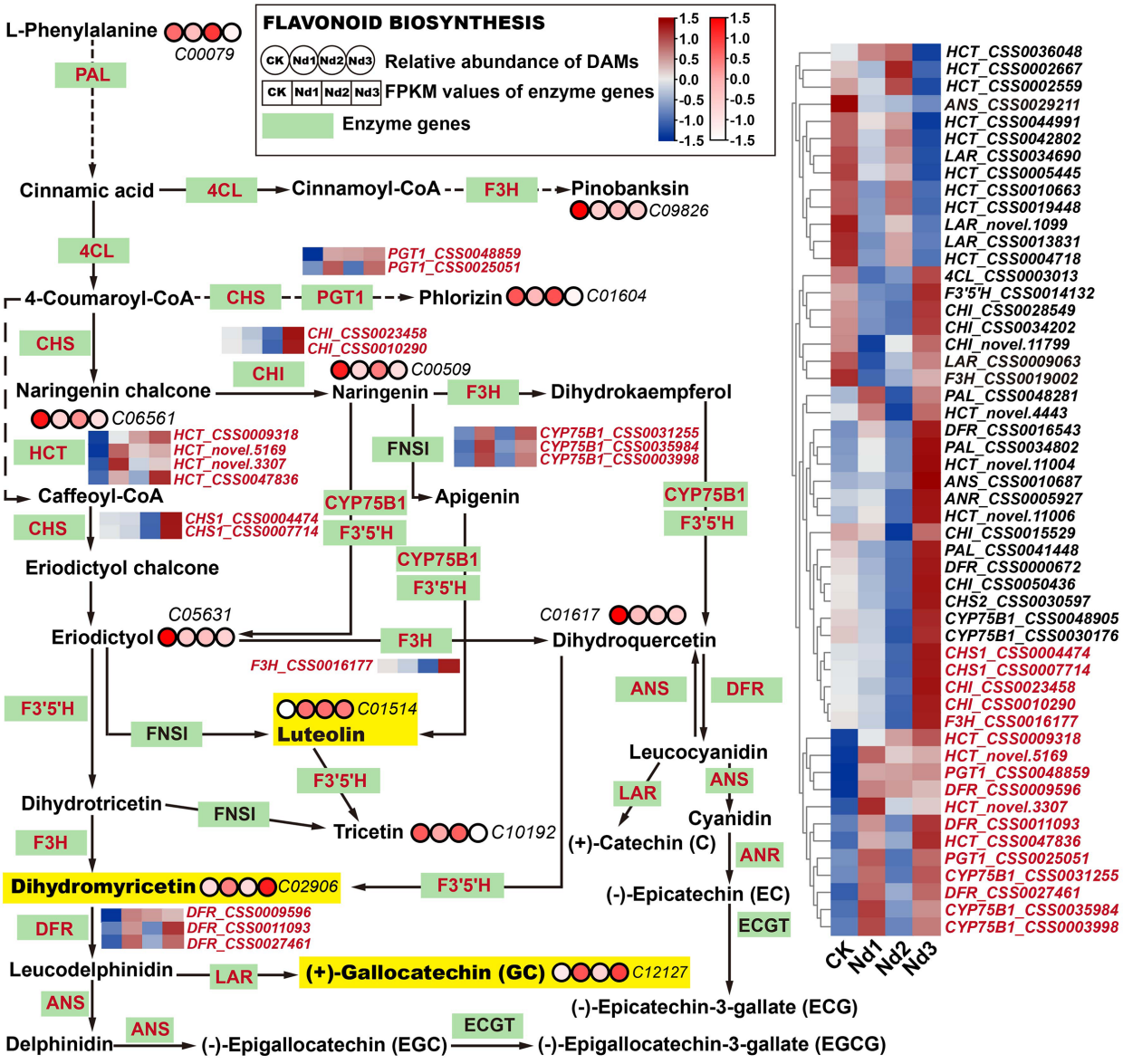

Fig. 4 Integrated analysis of flavonoid biosynthesis pathways' responses to nitrogen deficiency in new shoots. Green rectangular nodes represent enzyme genes annotated in KEGG pathways, with red labels indicating significantly DEGs ($|\log_2 FC| \geq 1$, FDR < 0.05). Red circular nodes indicate metabolites' relative abundance (KEGG IDs are specified, e.g., C00079), with darker red reflecting higher abundance. In the heatmap, genes in red show upregulated trends across nitrogen deprivation stages (CK→Nd3). Metabolites in yellow exhibit significant accumulation versus the controls ($\log_2 FC > 1.0$). All data were normalized via *Z*-score transformation in TBtools.

Metabolic reprogramming of jasmonic acid biosynthesis under nitrogen deficiency

Under nitrogen-deficient conditions, the new shoots of tea plants exhibited the significant accumulation of jasmonic acid (JA) and JA-Ile, as illustrated in Fig. 5. Compared with the control (CK), JA levels increased by 5.35-, 4.20-, and 3.61-fold at the Nd1, Nd2, and Nd3 stages (Supplementary Fig. S10), respectively, whereas JA-Ile levels rose even more markedly by 8.72-, 6.95-, and 20.19-fold over the same periods. Further transcriptomic analysis identified 19 DEGs (FPKM > 10) associated with the jasmonate pathway, among which 10 were upregulated. Seven of these upregulated genes are likely involved in JA and JA-Ile accumulation, including *Phospholipase A1(DAD1_CSS0045576), Lipoxygenase (LOX2S_CSS0021769), Jasmonic acid-amino synthetase (JAR4_CSS0032243), Jasmonate ZIM domain-containing proteins (JAZ_CSS0010510, JAZ_CSS0031905),* and the TF *MYC2 (MYC2_CSS0047466, MYC2_CSS0005453).*

These expression changes indicate that nitrogen deficiency activates the jasmonate biosynthesis pathway at multiple regulatory nodes: The initial steps mediated by DAD1 and LOX2S, conjugation to isoleucine by JAR4, and transcriptional activation via MYC2, potentially accompanied by feedback regulation involving JAZ repressors. The strong induction of JA-Ile in particular suggests enhanced jasmonate signaling, which may coordinate stress adaptation and resource reallocation in tea shoots under low nitrogen availability. In summary, nitrogen deficiency drives the upregulation of key jasmonate pathway genes, leading to pronounced accumulation of JA and JA-Ile, a response that likely facilitates stress adaptation through hormone-mediated transcriptional reprogramming.

Construction of the transcriptional regulatory network of characteristic metabolites in tea shoots under nitrogen-deficient conditions using WGCNA

Nitrogen deficiency triggered a systemic reprogramming of metabolism in tea shoots, as shown by the integrated transcriptomic and metabolomic analyses. To validate the transcriptome's reliability, qRT-PCR confirmed strong correlations (r > 0.5) for six key genes involved in nitrogen utilization and metabolite synthesis (Supplementary Fig. S11). WGCNA identified 10 co-expression modules

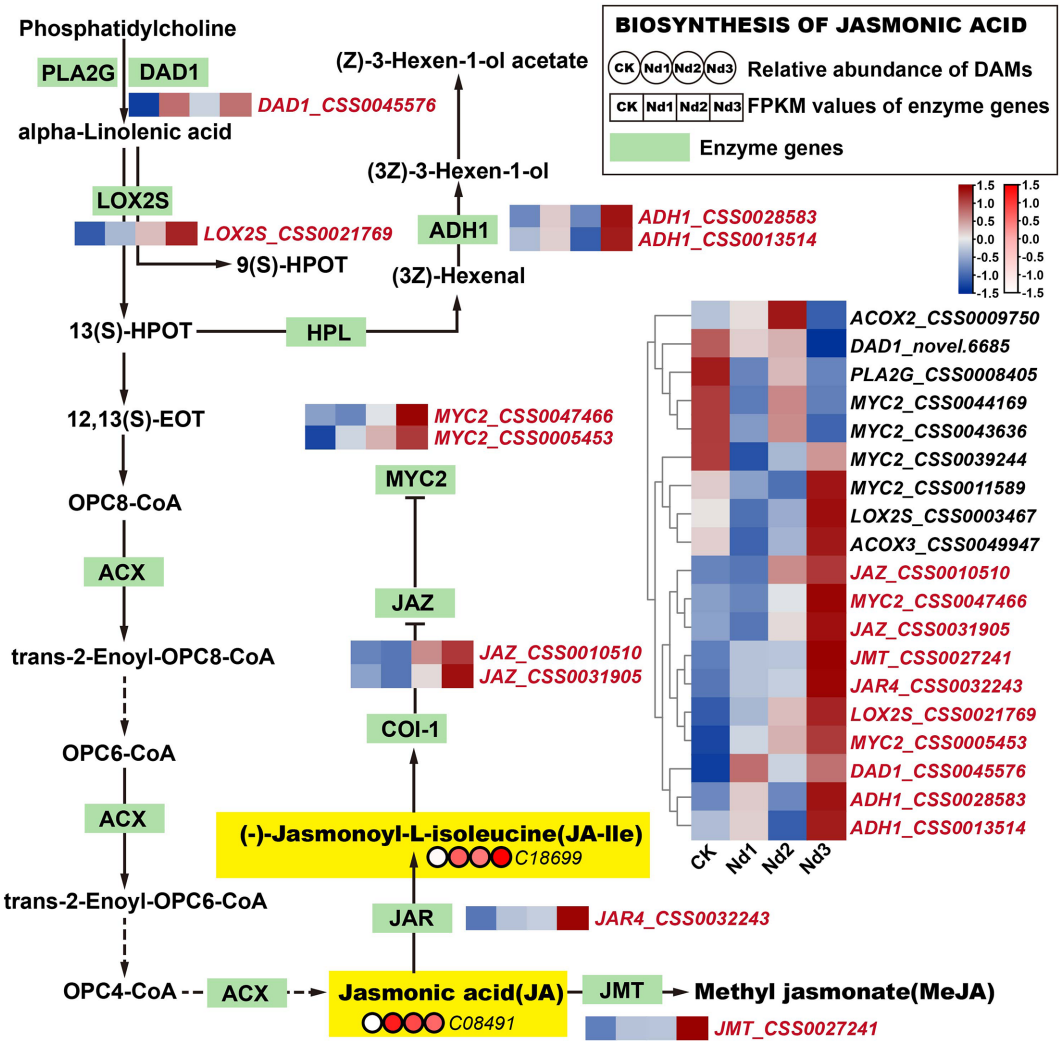

Fig. 5 Integrated analysis of the JA biosynthesis pathway's responses to nitrogen deficiency. Green rectangular nodes represent KEGG-annotated genes, with red labels marking significantly DEGs ($|\log_2 FC| \geq 1$, FDR < 0.05). Red circular nodes indicate metabolites' relative abundance (e.g., C08491 = JA), with darker red denoting higher abundance. In the heatmap, genes in red show upregulated expression trends across nitrogen deprivation stages (CK→Nd3). Metabolites in yellow exhibit significant accumulation versus the controls ($\log_2 FC > 1.0$). (-)-Jasmonoyl-L-isoleucine, JA-Ile; jasmonic acid, JA; methyl jasmonate, MeJA; total polyphenol content, TP. All data were normalized via *Z*-score transformation in TBtools.

from 7,945 genes (Fig. 6a, Supplementary Fig. S12), with distinct temporal dynamics: The red module showed progressive upregulation under prolonged stress, whereas the turquoise and black modules exhibited overall downregulation.

Global metabolic profiling highlighted 22 characteristic metabolites that were significantly altered under nitrogen stress, including defense signals (e.g., JA and (E)-2-hexenal), quality components (e.g., theanine and caffeine), and antioxidants (e.g., luteolin and ECG). Correlation analysis revealed that 9 of the 10 modules were strongly associated ($r > 0.60$, $p < 0.05$) with these metabolites (Fig. 6b). For instance, the red module correlated with luteolin and JA-Ile, indicating a coordinated stress response; the blue module was linked to theophylline and ECG, suggesting secondary metabolite adaptation; and the turquoise module was associated with abscisic acid and carbohydrate metabolites, reflecting energy reallocation. Notably, the red and blue modules emerged as central regulators of adaptation to nitrogen deficiency. Genes within these modules were enriched in the plant hormone signaling, flavonoid biosynthesis, and phenylpropanoid metabolism pathways. Hub genes such as *MYC2*, *JAZ*, and *CYP75B1* were identified as potential drivers of jasmonate and flavonoid accumulation, underpinning the shift from growth-oriented to defense-oriented metabolism.

The TF–gene–metabolite regulatory network in new shoots under nitrogen-deficient conditions

Integrated transcriptomic and metabolomic analyses were used to construct a transcriptional regulatory network in tea shoots under nitrogen deficiency, focusing on key modules identified through WGCNA. This study aimed to elucidate the active adaptive mechanisms by which tea plants prioritize defense-oriented metabolism over growth-related quality components under nutrient stress. On the basis of the the kWithin value (sum of intramodular connectivity), the top 50 genes from each module were selected for constructing the co-expression network. Hub genes and TFs with FPKM > 10 and high connectivity were further filtered using KEGG enrichment pathways (Fig. 7). The analysis specifically targeted the red module (MEred), strongly associated with luteolin and JA-Ile, and the green module (MEgreen), strongly linked to γ-aminobutyric acid (GABA), to uncover the core regulatory strategies.

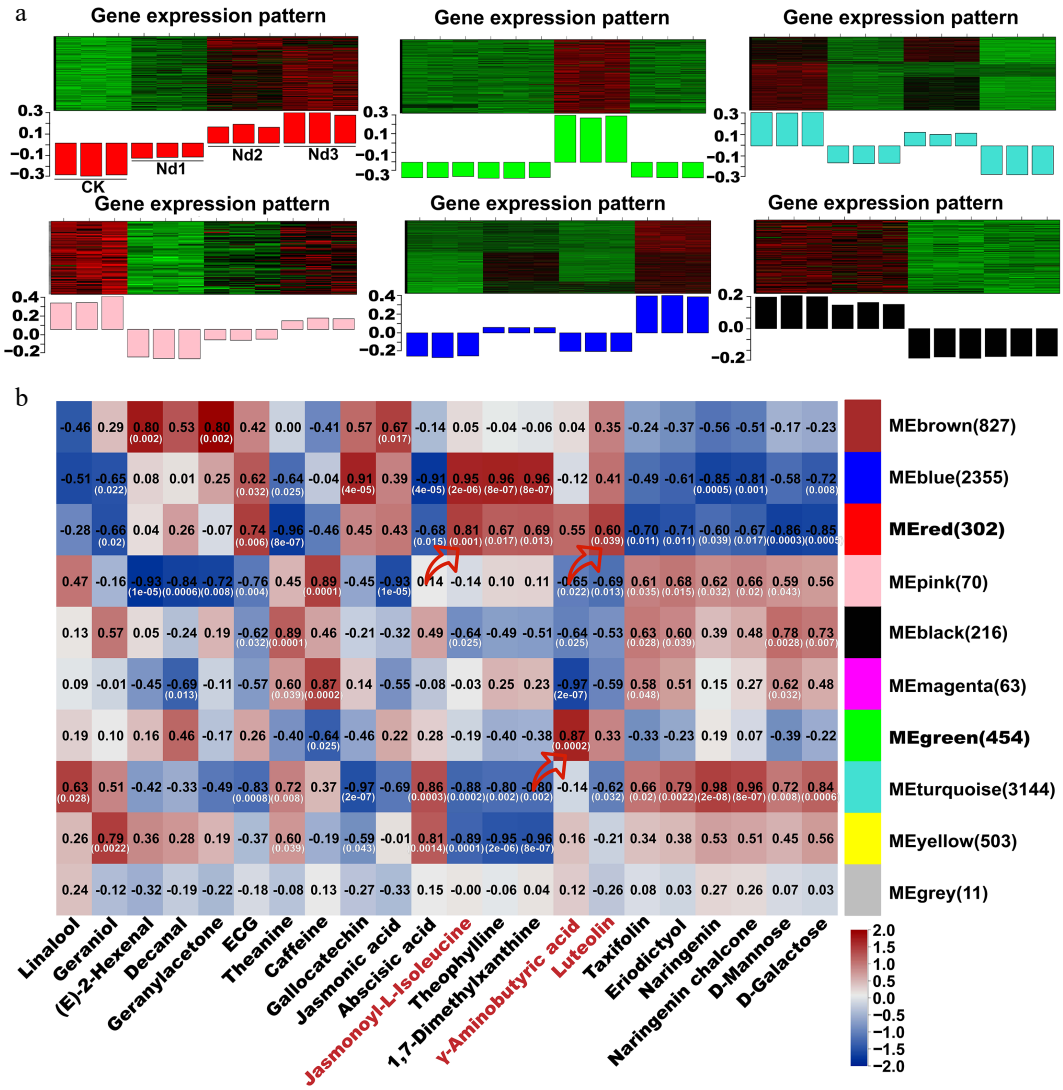

Fig. 6 WGCNA co-expression network of nitrogen deficiency responses in new shoots. (a) Heatmap of modules' eigengene expression trends across stages of nitrogen deficiency (CK-Nd3). (b) Module–trait correlation heatmap. Black numerals indicate Pearson's correlation coefficients (*r*) between the modules and target metabolites; white values in parentheses denote statistical significance (*p*-values). Red arrows highlight modules with strong positive correlations with the target metabolites ($r > 0.60$, $p < 0.05$).

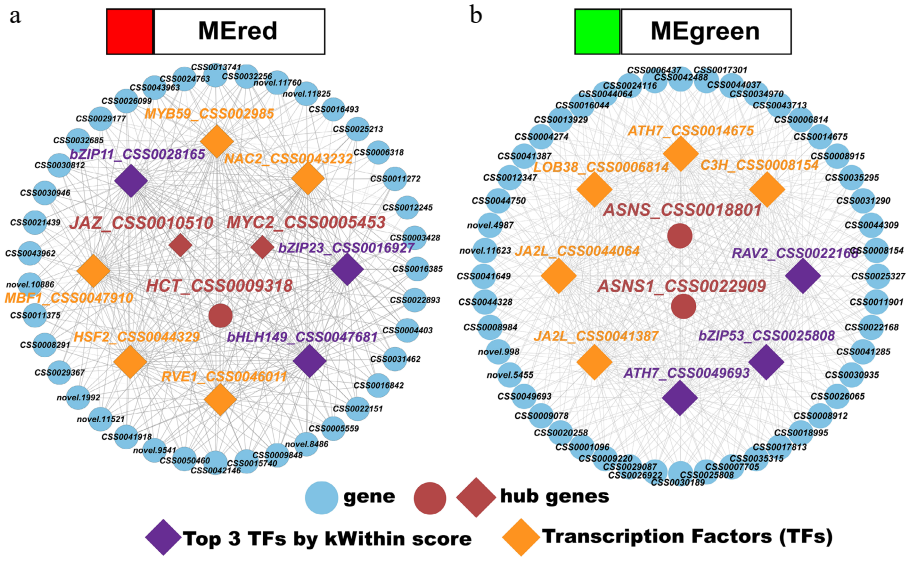

Fig. 7 (a), (b) Transcription factor–gene regulatory networks for the red and green modules.

Red module (MEred): The JA-Ile and luteolin accumulation hub

In the red module, three hub genes and eight potential regulatory TFs were identified. The top transcription factors according to the kWithin values were *bZIP11_CSS0028165, bHLH149_CSS0047681*, and *bZIP23_CSS0016927*. Notably, *MYC2_CSS0005453* and *JAZ_CSS0010510* exhibited a strong positive correlation with the accumulation of JA-Ile (r = 0.81, p < 0.001). This suggests that the TFs bZIP11, bZIP23, and bHLH149 may form a regulatory module (bZIP11/bZIP23/bHLH149-MYC2-JAZ) to promote JA-Ile synthesis, enhancing defense signaling under nitrogen deficiency. Additionally, the hub gene *HCT_CSS0009318* showed a significant positive correlation with lignan (r = 0.60, p < 0.05), indicating that these transcription factors may also regulate the expression of HCT to drive lignan accumulation, further supporting stress adaptation.

Green module (MEgreen): GABA synthesis and metabolic Homeostasis

In the green module, two hub genes (the asparagine synthase genes *ASNS_CSS0018801* and *ASNS1_CSS0022909*) were identified, along with eight potential regulatory TFs, including *RAV2_CSS0022168*, *bZIP53_CSS0025808,* and *ATH7_CSS0049693* (top kWithin values). The hub genes *ASNS* and *ASNS1* demonstrated a strong positive correlation with GABA accumulation (r = 0.87, p < 0.001). The TFs RAV2, bZIP53, and ATH7 likely form a RAV2/bZIP53/ATH7-ASNS module to upregulate GABA synthesis, facilitating carbon–nitrogen balance and cellular homeostasis under nitrogen stress.

Discussion

Increase in the carbon–nitrogen ratio and decline in quality of tea plant new shoots under nitrogen-deficient conditions

In this study, we found that nitrogen-deficient conditions significantly increased the carbon–nitrogen ratio (C/N), with the most pronounced change observed at the Nd1 stage (Fig. 1a). The C/N ratio is an important indicator of nitrogen use efficiency. In nature, species with a higher C/N ratio are generally able to survive in environments with limited nitrogen resources. A similar increase in the C/N ratio has been observed in crops like wheat and citrus under nitrogen-deficient conditions, which may be a plant adaptation strategy to improve nitrogen use efficiency[25–27]. Compared with the 15-d and 30-d nitrogen deficiency stages, the change at Day 7 might be related to the plant's early response to nitrogen deprivation. Related studies have shown that, under short-term nitrogen starvation, amino acid metabolism in the roots is significantly affected, whereas under long-term nitrogen-deficient conditions, the changes in roots' amino acid metabolism are smaller, with the main trend being a reduction in proteins that defend against pathogens[28]. Additionally, studies have found that under nitrogen-deficient conditions in five barley varieties, *HvNRT2.1*, *HvNRT2.2,* and *HvNRT2.4* were strongly induced by NO_3^- within 7 and 14 d of the nitrogen deficiency treatment, reaching peak levels at these time points[29]. This suggests that under long-term nitrogen-deficient conditions, plants may exhibit more generalized stress responses. In the early stages of nitrogen-deficient conditions, plants may respond to the nitrogen shortage by increasing carbon accumulation, which leads to a sharp rise in the C/N ratio. Over time, however, the plant's adaptation mechanisms gradually change, and the magnitude of the change in the C/N ratio becomes relatively smaller.

Nitrogen-deficient conditions and the decline in the quality in shoots of tea plants

The contents of chlorophyll and theanine decrease, with the lowest levels observed at the Nd3 stage (Fig. 1b). At the same time, one important indicator of tea quality, namely the ratio of total phenols to amino acids (TP/FAA), increases continuously with the growth of shoots under nitrogen-deficient conditions (Fig. 1c). Under nitrogen-deficient conditions, the total amounts of caffeine and catechins significantly decline, reaching their lowest levels at the Nd2 stage. Among the catechin monomers, ECG significantly increases at the Nd1 stage, whereas the content of epigallocatechin gallate (EGCG) reaches its lowest point at this stage (Fig. 1d). This result is consistent with our previous 30-d nitrogen deficiency experiment on the *Camellia sinensis* 'Jinxuan' variety (JX)[30], which showed that nitrogen-deficient conditions reduced the chlorophyll and water-soluble extract contents in JX tea shoots, and nitrogen

was primarily accumulated in the roots. Nitrogen-deficient conditions also led to a significant decrease in caffeine content, as well as in the total theanine and catechins in the shoots and roots. However, the accumulation of EGCG in JX tea shoots increased, suggesting that different tea varieties may exhibit varying tolerance and response mechanisms to nitrogen-deficient conditions. Related studies have also pointed out that nitrogen-deficient conditions inhibits tea plant growth, possibly through changes in nitrogen metabolism, as well as the expression of DEGs related to photosynthetic performance, transport activity, and redox processes[31]. Nitrogen-deficient conditions significantly reduced the nitrogen content, dry weight, chlorophyll content, theanine content, and the activity of nitrogen metabolism-related enzymes in tea leaves but increased the total flavonoid and polyphenol contents[7]. Therefore, nitrogen-deficient conditions led to a reduction in total free amino acids, theanine, caffeine, and chlorophyll in the shoots while increasing the total polyphenol content. However, the results regarding changes in catechin content are inconsistent. Studies have shown that when nitrate (NO_3^-) is used as the nitrogen source, the catechin content increases, and most of the genes related to catechin biosynthesis are upregulated under nitrogen-deficient conditions[10]. The differences in catechin responses across studies may be related to variations in the experimental conditions, tea plant varieties, nitrogen sources, and experimental stages. For instance, in the JX variety, the increased accumulation of EGCG suggests that different tea plant varieties may respond differently to nitrogen-deficient conditions[30]. Furthermore, differences in nitrogen sources (such as NO_3^- versus NH_4^+) may also affect the catechin synthesis pathway, leading to different outcomes[32]. Therefore, further exploration of the catechin responses in different tea plant genotypes under nitrogen-deficient conditions is of great significance for selecting tea plants with high nitrogen-use efficiency.

Accumulation of aldehyde compounds in tea plant shoots under nitrogen-deficient conditions

Under nitrogen-deficient conditions, the proportion of aldehyde compounds in the shoots significantly increased, especially the concentration of (E)-2-hexenal, which was, on average, 42.88% higher, whereas the concentration of decanal increased by 138.11%, with the greatest increase occurring at the Nd1 stage (Fig. 2a). These aldehydes and alcohols are mainly synthesized via plant fatty acid metabolism, with the primary sources being linoleic acid and linolenic acid. In this process, fatty acids are deoxygenated by the action of lipoxygenase (LOX), forming 13- or 9-hydroperoxy linoleic acid. Subsequently, 13-hydroperoxy linoleic acid can be cleaved by hydroperoxide lyase (HPL) to produce C6 aldehydes such as hexanal or (3Z)-hexenal. Because of the instability of (3Z)-hexenal, it easily undergoes isomerization to convert into the (2E)-en-aldehyde isomer. Therefore, (Z)-3-hexenal readily isomerizes into (E)-2-hexenal[33]. Studies have shown that the release of (E)-2-hexenal is influenced by various stresses, such as insect damage, high temperatures, and other factors[34–36]. In our preliminary research, although it was observed that JX accumulated (E)-2-hexenal under nitrogen-deficient conditions, the accumulation level was lower compared with the variety in this study[30]. Additionally, rosemary has been found to significantly induce the accumulation of aldehyde compounds, including (E)-2-hexenal, leaf alcohol, sorbaldehyde, and n-decanal, under drought stress[37]. Furthermore, fresh tea leaf disruption induces > 1,000-fold increases in the (E)-2-hexenal and (Z)-3-hexenal content. The newly identified *Camellia sinensis* hexenal isomerase (*CsHI*) irreversibly converts (Z)-3-hexenal to (E)-2-hexenal. Although nonbiological stresses (e.g., low temperature, dehydration) have minimal effects on (E)-2-hexenal levels in intact leaves, transcriptional regulation of *CsHI* directly modulates the enantiomer ratio in broken tissues[38]. Notably, (E)-2-hexenal contributes significantly to the characteristic green leaf odor associated with plant volatiles. Although these odors may serve to attract pollinators or warn pests in the natural environment of plants, excessive accumulation in tea leaves can cause the tea aroma to become overly 'green', masking the floral, fruity, or other unique scent components that tea is meant to have[38]. Tea cultivars that are suitable for oolong tea, such as *Camellia sinensis* 'Lingtou Dancong', as used in this study, typically exhibit sweet and floral characteristics[5]. Therefore, this overly intense grassy aroma not only deviates from the traditional aromatic profile of the tea but may also mask other more valuable aromatic components.

The TF–gene–metabolite regulatory network in tea plant shoots under nitrogen-deficient conditions

This study demonstrates that tea shoots adapt to nitrogen-deficient environments by increasing the accumulation of luteolin, JA-Ile, and GABA. Luteolin, a natural flavonoid compound, has been shown to play an important role in plants' stress resistance. For instance, melatonin enhances luteolin biosynthesis by inducing the expression of the CcPCL1 TF, thereby improving plants' salt tolerance[39]. Furthermore, multiple studies have confirmed that nitrogen-deficient conditions lead to an increase in the accumulation of luteolin, suggesting that plants enhance luteolin levels in response to nitrogen limitations[40,41], consistent with the findings of this study. JA-Ile, a key bioactive substance of JA, plays a crucial role in plants' stress responses by activating the core JA signaling pathway through binding with the SCFCOI1-JAZ co-receptor[42]. For example, nitrogen-deficient conditions enhances eggplant's defense against western flower thrips, demonstrating the critical role of JA-Ile under nitrogen-limited conditions[43]. In this study, we found that the TFs bZIP11, bZIP23, and bHLH149 strongly correlated with *HCT* and *MYC2-JAZ*, regulating the accumulation of luteolin and JA-Ile under nitrogen-deficient conditions (Fig. 7). Previous studies have shown that bZIP11 activates auxin transcription through histone acetylation mechanisms, promoting the accumulation of sugar in tomato fruit and inhibiting plant growth[44,45]. bZIP23 regulates drought resistance genes and absciscic acid signaling in rice, participating in the regulation of salt and osmotic stress tolerance[46–48]. bHLH149 positively regulates disease resistance in cassava and activates the *LCYB* gene during postharvest ripening in kiwifruit, controlling carotenoid synthesis[49,50]. Furthermore, HCT, a key enzyme in lignin monomer synthesis, shows a decrease in expression with increased concentrations of p-coumaroylquinic acid and caffeoylquinic acid[51]. Notably, under nitrogen-deficient conditions, bHLH130 is significantly positively correlated with the expression of *HCT (MD14G1155800)* but does not bind to the *MhHCT* promoter[51]. For plant growth under nitrogen, phosphorus, and potassium deficiency stress, genes such as *NPF7.3*, *GlpT4*, *HAK24*, *HAK5*, *MRP2*, *bZIP77*, and *bZIP53* are potential candidates for regulating root growth in maize[52]. Although luteolin demonstrates potential in plant stress resistance, its specific regulatory mechanisms across different biological processes have not yet been fully elucidated. Additionally, members of the JAZ protein family regulate hormone signaling by interacting with the TF MYC2 in plants like *Arabidopsis*, with the *MYC2–PUB22–JAZ4* module playing a critical role in jasmonic acid signaling in tomato[53]. Therefore, investigating the roles of these two modules in tea plant shoots' responses

to nitrogen-deficient conditions may reveal metabolic regulatory pathways involved in the plant's adaptation to nitrogen limitations. Nitrogen-deficient conditions typically affects plants' growth and metabolic processes, with luteolin and JA-Ile both being closely associated with stress responses, potentially participating in regulating plants' adaptation to nitrogen-deficient conditions.

GABA, a nonproteinogenic amino acid, accumulates under various stress conditions and plays a critical role in adaptation[54]. Studies indicate that in nitrogen-deficient tea plants, GABA accumulation significantly increases in response to both biotic and abiotic stresses. Furthermore, the synthesis of GABA is more pronounced in nitrogen-tolerant varieties, suggesting its potential role in enhancing nitrogen tolerance in tea plants[12]. Our findings suggest that the *RAV2/bZIP53/ATH7-ASNS* module may regulate the accumulation of GABA (Fig. 7). The S1 group basic leucine zipper TF bZIP53 modulates primary metabolic reprogramming under low-energy stress by heterodimerizing to activate the transcription of key metabolic genes, including *Asparagine synthetase 1* (*Asn1*) and *proline dehydrogenase* (*PDH*), thereby regulating the biosynthesis of proline, asparagine, and branched-chain amino acids. Although single-gene deletion of *bZIP53* minimally affects starvation-induced transcriptional responses, its collaborative function with other bZIP proteins is essential for sustaining plants' tolerance to energy deprivation. These findings collectively establish bZIP53 as a central regulatory node in low-energy signaling networks, orchestrating metabolic remodeling to ensure plants' survival under starvation conditions[55]. In conclusion, by regulating the synthesis of these metabolites under nitrogen-deficient conditions, tea plants may enhance their ability to adapt to nitrogen-limited stress. Despite the valuable insights provided by this study, several limitations must be acknowledged. First, the small sample size in the WGCNA analysis may affect the stability and reliability of network construction. Second, the hydroponic environment used in this study differs from natural field conditions, which may limit the applicability of our findings to field-grown tea plants. Additionally, the reliance on transcriptomic data for identifying regulatory relationships is correlative, and further functional studies are necessary to confirm direct regulatory links. Future research with larger sample sizes and validation in natural environments is needed to enhance and expand upon these results.

Conclusions

Integrated multi-omics analysis systematically revealed that nitrogen deficiency induces an adaptive reprogramming in the new shoots of tea plants, shifting from a growth-oriented to a defense-oriented metabolic phenotype through coordinated regulation of gene expression and metabolite synthesis. Nitrogen deficiency significantly increased the C/N and phenol-to-amino acid (TP/AA) ratios, leading to a marked decline in quality-related components such as theanine and caffeine, while activating the accumulation of defense metabolites including JA-Ile (up to 20.19-fold), luteolin, and GABA. This metabolic reprogramming was primarily driven by three core transcriptional regulatory modules: The bZIP11/23/bHLH149-HCT module regulating luteolin synthesis, the bZIP11/23/bHLH149-MYC2-JAZ module promoting the accumulation of JA-Ile, and the RAV2/bZIP53/ATH7-ASNS module facilitating GABA production. These modules function synergistically to redirect carbon flux from quality-associated metabolism toward defense-related secondary metabolism, reflecting a multi-pathway adaptation strategy involving hormone signaling, antioxidant response, and nitrogen rebalancing under nitrogen stress. This study provides novel insights into the molecular mechanisms of nitrogen use efficiency in tea plants and identifies key candidate genes (e.g., *MYC2*, *bZIP53*) and metabolic markers (e.g., JA-Ile, luteolin) for breeding tea varieties with improved nitrogen adaptation.

Author contributions

The authors confirm contributions to the paper as follows. Study conception and design, and manuscript editing and revision: Qiu Z, Liu R, and Sun B. Data analysis: Qiu Z, Li A. Constructing figures and the manuscript: Qiu Z, Lin X, and Yao J. Performing experiments: Qiu Z, Li A, and Yang Y. Providing materials and resources: Liu S and Zheng P. All authors reviewed the results and approved the final version of the manuscript.

Data availability

Raw RNA-Seq data generated in this study have been deposited in the NCBI Short Read Archive (SRA) under accession number PRJNA1269270. Raw metabolomic data have been deposited in the National Genomics Data Center (https://ngdc.cncb.ac.cn) under accession number OMIX010416. All raw datasets, including the omics data, are available from the corresponding author upon reasonable request.

Acknowledgments

The authors are indebted to the entire staff of the research group for their active role in acquiring the experimental data. This work was supported by the Innovative Team Construction Project of the Modern Agricultural Industrial Technology System in Guangdong Province with agricultural products as the unit (tea industry technology system) (2024CXTD11).

Conflict of interest

The authors declare that they have no conflict of interest.

Supplementary information accompanies this paper online at: https://doi.org/10.48130/bpr-0025-0041.

Dates

Received 14 October 2025; Revised 3 December 2025; Accepted 5 December 2025; Published online 16 March 2026

References

[1] Zhao S, Cheng H, Xu P, Wang Y. 2023. Regulation of biosynthesis of the main flavor-contributing metabolites in tea plant (*Camellia sinensis*): a review. *Critical Reviews in Food Science and Nutrition* 63:10520–10535

[2] Chen Y, Wang F, Wu Z, Jiang F, Yu W, et al. 2021. Effects of long-term nitrogen fertilization on the formation of metabolites related to tea quality in subtropical China. *Metabolites* 11:146

[3] Dong F, Hu J, Shi Y, Liu M, Zhang Q, et al. 2019. Effects of nitrogen supply on flavonol glycoside biosynthesis and accumulation in tea leaves (*Camellia sinensis*). *Plant Physiology and Biochemistry* 138:48–57

[4] Zhao S, Bai Y, Jin Z, Long L, Diao W, et al. 2023. Effects of the combined application of nitrogen and selenium on tea quality and the expression of genes involved in nitrogen uptake and utilization in tea cultivar 'Chuancha No. 2'. *Agronomy* 13:2997

[5] Qiu Z, Liao J, Chen J, Li A, Lin M, et al. 2024. Comprehensive analysis of fresh tea (*Camellia sinensis* cv. Lingtou Dancong) leaf quality under different nitrogen fertilization regimes. *Food Chemistry* 439:138127

[6] Hu S, Zhang M, Yang Y, Xuan W, Zou Z, et al. 2020. A novel insight into nitrogen and auxin signaling in lateral root formation in tea plant [*Camellia sinensis* (L.) O. Kuntze]. *BMC Plant Biology* 20:232

[7] Lin ZH, Chen CS, Zhong QS, Ruan QC, Chen ZH, et al. 2021. The GC-TOF/MS-based metabolomic analysis reveals altered metabolic profiles in nitrogen-deficient leaves and roots of tea plants (*Camellia sinensis*). *BMC Plant Biology* 21:506

[8] Samarina L, Malyukova L, Wang S, Li Y, Doroshkov A, et al. 2024. Nitrogen deficiency differentially affects lignin biosynthesis genes and flavanols accumulation in tolerant and susceptible tea genotypes (*Camellia sinensis* (L.) Kuntze). *Plant Stress* 14:100581

[9] Huang H, Yao Q, Xia E, Gao L. 2018. Metabolomics and transcriptomics analyses reveal nitrogen influences on the accumulation of flavonoids and amino acids in young shoots of tea plant (*Camellia sinensis* L.) associated with tea flavor. *Journal of Agricultural and Food Chemistry* 66:9828–9838

[10] Wang Y, Wang YM, Lu YT, Qiu QL, Fan DM, et al. 2021. Influence of different nitrogen sources on carbon and nitrogen metabolism and gene expression in tea plants (*Camellia sinensis* L.). *Plant Physiology and Biochemistry* 167:561–566

[11] Li F, Li H, Dong C, Yang T, Zhang S, et al. 2020. Theanine transporters are involved in nitrogen deficiency response in tea plant (*Camellia sinensis* L.). *Plant Signaling & Behavior* 15:1728109

[12] Ruan L, Wei K, Li J, He M, Wu L, et al. 2022. Responses of tea plants (*Camellia sinensis*) with different low-nitrogen tolerances during recovery from nitrogen deficiency. *Journal of the Science of Food and Agriculture* 102:1405–1414

[13] Liu MY, Burgos A, Zhang Q, Tang D, Shi Y, et al. 2017. Analyses of transcriptome profiles and selected metabolites unravel the metabolic response to NH_4^+ and NO_3^- as signaling molecules in tea plant (*Camellia sinensis* L.). *Scientia Horticulturae* 218:293–303

[14] Lichtenthaler HK. 1987. [34] Chlorophylls and carotenoids: pigments of photosynthetic biomembranes. In: *Plant Cell Membranes: Methods in Enzymology*. eds. Packer L, Douce R. Amsterdam: Elsevier; pp. 350–382 doi: 10.1016/0076-6879(87)48036-1

[15] Wang JY, Chen JD, Wang SL, Chen L, Ma CL, et al. 2020. Repressed gene expression of photosynthetic antenna proteins associated with yellow leaf variation as revealed by bulked segregant RNA-seq in tea plant *Camellia sinensis*. *Journal of Agricultural and Food Chemistry* 68:8068–8079

[16] Salo-väänänen PP, Koivistoinen PE. 1996. Determination of protein in foods: comparison of net protein and crude protein (N × 6.25) values. *Food Chemistry* 57:27–31

[17] Bicharanloo B, Bagheri Shirvan M, Dijkstra FA. 2022. Decoupled cycling of carbon, nitrogen, and phosphorus in a grassland soil along a hillslope mediated by clay and soil moisture. *CATENA* 219:106648

[18] Chen J, Mei S, Zheng P, Guo J, Zeng Z, et al. 2023. A multi-omics view of the preservation effect on *Camellia sinensis* leaves during low temperature postharvest transportation. *LWT* 178:114614

[19] Chen P, Cai J, Zheng P, Yuan Y, Tsewang W, et al. 2022. Quantitatively unravelling the impact of high altitude on oolong tea flavor from *Camellia sinensis* grown on the plateaus of Tibet. *Horticulturae* 8:539

[20] Hu CJ, Li D, Ma YX, Zhang W, Lin C, et al. 2018. Formation mechanism of the Oolong tea characteristic aroma during bruising and withering treatment. *Food Chemistry* 269:202–211

[21] Wang P, Gu M, Shao S, Chen X, Hou B, et al. 2022. Changes in non-volatile and volatile metabolites associated with heterosis in tea plants (*Camellia sinensis*). *Journal of Agricultural and Food Chemistry* 70:3067–3078

[22] Lin N, Liu X, Zhu W, Cheng X, Wang X, et al. 2021. Ambient ultraviolet B signal modulates tea flavor characteristics via shifting a metabolic flux in flavonoid biosynthesis. *Journal of Agricultural and Food Chemistry* 69:3401–3414

[23] Ogata H, Goto S, Sato K, Fujibuchi W, Bono H, et al. 1999. KEGG: Kyoto Encyclopedia of Genes and Genomes. *Nucleic Acids Research* 27:29–34

[24] Kanehisa M. 2019. Toward understanding the origin and evolution of cellular organisms. *Protein Science* 28:1947–1951

[25] Liu X, Wang S, Deng X, Zhang Z, Yin L. 2020. Comprehensive evaluation of physiological traits under nitrogen stress and participation of linolenic acid in nitrogen-deficiency response in wheat seedlings. *BMC Plant Biology* 20:501

[26] Zhang J, He N, Liu C, Xu L, Chen Z, et al. 2020. Variation and evolution of C:N ratio among different organs enable plants to adapt to N-limited environments. *Global Change Biology* 26:2534–2543

[27] Huang WT, Zheng ZC, Hua D, Chen XF, Zhang J, et al. 2022. Adaptive responses of carbon and nitrogen metabolisms to nitrogen-deficiency in *Citrus sinensis* seedlings. *BMC Plant Biology* 22:370

[28] Møller ALB, Pedas P, Andersen B, Svensson B, Schjoerring JK, et al. 2011. Responses of barley root and shoot proteomes to long-term nitrogen deficiency, short-term nitrogen starvation and ammonium. *Plant, Cell & Environment* 34:2024–2037

[29] Hajibarat Z, Saidi A, Ghazvini H, Hajibarat Z. 2023. Comparative analysis of physiological traits and gene expression patterns in nitrogen deficiency among barley cultivars. *Journal of Genetic Engineering and Biotechnology* 21:110

[30] Qiu Z, Li A, Huang W, Chen J, Lin X, et al. 2024. Metabolic profiling reveal changes in shoots and roots of nitrogen-deficient tea plants (*Camellia sinensis* cv. Jinxuan). *Scientia Horticulturae* 337:113528

[31] Lin ZH, Chen CS, Zhao SQ, Liu Y, Zhong QS, et al. 2023. Molecular and physiological mechanisms of tea (*Camellia sinensis* (L.) O. Kuntze) leaf and root in response to nitrogen deficiency. *BMC Genomics* 24:27

[32] Tang D, Liu MY, Zhang Q, Ma L, Shi Y, et al. 2020. Preferential assimilation of NH_4^+ over NO_3^- in tea plant associated with genes involved in nitrogen transportation, utilization and catechins biosynthesis. *Plant Science* 291:110369

[33] Li J, Lin T, Ren D, Wang T, Tang Y, et al. 2021. Transcriptomic and metabolomic studies reveal mechanisms of effects of CPPU-mediated fruit-setting on attenuating volatile attributes of melon fruit. *Agronomy* 11:1007

[34] Hao X, Wang S, Fu Y, Liu Y, Shen H, et al. 2024. The WRKY46–MYC_2 module plays a critical role in E-2-hexenal-induced anti-herbivore responses by promoting flavonoid accumulation. *Plant Communications* 5:100734

[35] Ju YL, Yue XF, Zhao XF, Zhao H, Fang YL. 2018. Physiological, micromorphological and metabolomic analysis of grapevine (*Vitis vinifera* L.) leaf of plants under water stress. *Plant Physiology and Biochemistry* 130:501–510

[36] Loreto F, Barta C, Brilli F, Nogues I. 2006. On the induction of volatile organic compound emissions by plants as consequence of wounding or fluctuations of light and temperature. *Plant, Cell & Environment* 29:1820–1828

[37] Liu F, Zuo ZJ, Xu GP, Wu XB, Zheng J, et al. 2013. Physiological responses to drought stress and the emission of induced volatile organic compounds in *Rosmarinus officinalis*: physiological responses to drought stress and the emission of induced volatile organic compounds in *Rosmarinus officinalis*. *Chinese Journal of Plant Ecology* 37:454–463

[38] Chen C, Yu F, Wen X, Chen S, Wang K, et al. 2022. Characterization of a new (Z)-3: (E)-2-hexenal isomerase from tea (*Camellia sinensis*) involved in the conversion of (Z)-3-hexenal to (E)-2-hexenal. *Food Chemistry* 383:132463

[39] Song Z, Yang Q, Dong B, Li N, Wang M, et al. 2022. Melatonin enhances stress tolerance in pigeon pea by promoting flavonoid enrichment, particularly luteolin in response to salt stress. *Journal of Experimental Botany* 73:5992–6008

[40] Liu Q, Li L, Cheng H, Yao L, Wu J, et al. 2021. The basic helix-loop-helix transcription factor TabHLH1 increases chlorogenic acid and luteolin biosynthesis in *Taraxacum antungense* Kitag. *Horticulture Research* 8:195

[41] Li Z, Jiang H, Qin Y, Yan H, Jiang X, et al. 2021. Nitrogen deficiency maintains the yield and improves the antioxidant activity of *Coreopsis tinctoria* Nutt. *Bioscience, Biotechnology, and Biochemistry* 85:1492–1505

[42] Li M, Yu G, Cao C, Liu P. 2021. Metabolism, signaling, and transport of jasmonates. *Plant Communications* 2:100231

[43] Zheng Y, Liu Q, Shi S, Zhu X, Chen Y, et al. 2024. Nitrogen deficiency enhances eggplant defense against western flower thrips via the induction of the jasmonate pathway. *Plants* 13:273

[44] Weiste C, Pedrotti L, Selvanayagam J, Muralidhara P, Fröschel C, et al. 2017. The *Arabidopsis* bZIP11 transcription factor links low-energy signalling to auxin-mediated control of primary root growth. *PLoS Genetics* 13:e1006607

[45] Zhang Y, Li S, Chen Y, Liu Y, Lin Y, et al. 2022. Heterologous overexpression of strawberry bZIP11 induces sugar accumulation and inhibits plant growth of tomato. *Scientia Horticulturae* 292:110634

[46] Zong W, Tang N, Yang J, Peng L, Ma S, et al. 2016. Feedback regulation of ABA signaling and biosynthesis by a bZIP transcription factor targets drought-resistance-related genes. *Plant Physiology* 171:2810–2825

[47] Wang T, Li XK, Liu X, Yang XQ, Li YJ, et al. 2023. Rice glycosyltransferase gene *UGT2* functions in salt stress tolerance under the regulation of bZIP23 transcription factor. *Plant Cell Reports* 42:17–28

[48] Ma Y, Wu Z, Dong J, Zhang S, Zhao J, et al. 2023. The 14-3-3 protein OsGF14f interacts with OsbZIP23 and enhances its activity to confer osmotic stress tolerance in rice. *The Plant Cell* 35:4173–4189

[49] Cui M, An F, Chen S, Qin X. 2024. Expression pattern and functional analysis of MebHLH149 gene in response to cassava bacterial blight. *Plants* 13:2422

[50] Gan Z, Zhang Y, Yang C, Cao Q, Zhu L, et al. 2025. A kiwifruit bHLH149 transcription factor modulates carotenoid biosynthesis by directly activating *LCYB* during postharvest ripening. *Fruit Research* 5:e003

[51] Wang X, Chai X, Gao B, Deng C, Günther CS, et al. 2023. Multi-omics analysis reveals the mechanism of bHLH130 responding to low-nitrogen stress of apple rootstock. *Plant Physiology* 191:1305–1323

[52] Ma N, Dong L, Lü W, Lü J, Meng Q, et al. 2020. Transcriptome analysis of maize seedling roots in response to nitrogen-, phosphorus-, and potassium deficiency. *Plant and Soil* 447:637–658

[53] Wu S, Hu C, Zhu C, Fan Y, Zhou J, et al. 2024. The MYC_2–PUB22–JAZ4 module plays a crucial role in jasmonate signaling in tomato. *Molecular Plant* 17:598–613

[54] Yuan D, Wu X, Gong B, Huo R, Zhao L, et al. 2023. GABA metabolism, transport and their roles and mechanisms in the regulation of abiotic stress (hypoxia, salt, drought) resistance in plants. *Metabolites* 13:347

[55] Dietrich K, Weltmeier F, Ehlert A, Weiste C, Stahl M, et al. 2011. Heterodimers of the *Arabidopsis* transcription factors bZIP1 and bZIP53 reprogram amino acid metabolism during low energy stress. *The Plant Cell* 23:381–395